1310 nm Narrow Linewidth Laser Assisted by the Feedback of Double-FBGs

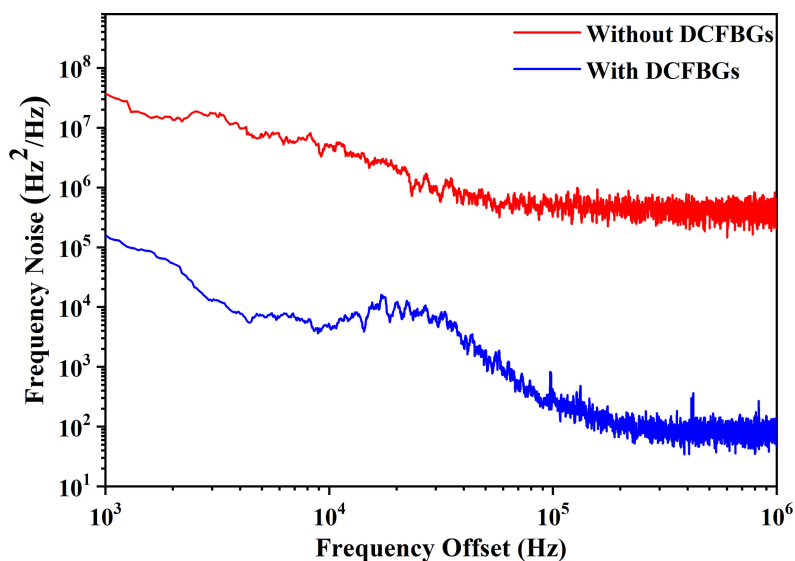Paul Ikechukwu Iroegbu, *Student Member, IEEE*
Min Liu
Tianyi Lan
Dan Wang
Haonan Han
Yujia Li
Yulong Cao
Fuhui Li
Udochukwu Frank Iroegbu
Ligang Huang
Guolu Yin
Tao Zhu

1310 nm Narrow Linewidth Laser Assisted by the Feedback of Double-FBGs

Paul Ikechukwu Iroegbu [1,2] ***Student Member, IEEE*, Min Liu,**[1,2]
Tianyi Lan,[1] **Dan Wang,**[1] **Haonan Han,**[1,2] **Yujia Li** [1], **Yulong Cao,**[1]
Fuhui Li,[1] **Udochukwu Frank Iroegbu,**[3] **Ligang Huang,**[1]
Guolu Yin [1], **and Tao Zhu** [1]

[1]Key Laboratory of Optoelectronic Technology and Systems (Ministry of Education), Chongqing University, Chongqing 400044, China
[2]School of Microelectronics and Communication Engineering, Chongqing University, Chongqing 400044, China
[3]Department of Management Science and Engineering, Xidian University, Xian 710126, China

Abstract: Narrow linewidth lasers with kHz or Hz have attracted tremendous attention due to their versatile applications in optical fiber sensing and optical fiber communication fields. This is because the efficiency of these fields depends on the quality of the laser source employed. This paper proposes, simulates, and experimentally demonstrates a dual cavity fiber Bragg grating assisted feedback structure. Based on the Rayleigh backscattering mechanism, Vernier effect, and interference phenomenon, the 2 MHz linewidth of a 1310 nm distributed feedback laser was highly compressed to ~580 Hz with a side mode suppression ratio as high as 34 dB. The output power of our proposed laser was found to be stable at 2.0 mW. The outcome of this work presents an idea centered on laser linewidth compression that applies to DFB lasers operating at various wavelengths.

Index Terms: Distributed feedback laser, linewidth compression, rayleigh backscattering, vernier effect.

1. Introduction

Single longitudinal mode (SLM) distributed feedback (DFB) lasers linewidth suppression to kHz or Hz is a significant research area owing to its versatile application. SLM-DFB laser is applicable in numerous fields, including- high precision optical measurement systems [1]–[6], high data rate optical coherent communications [7], [8], laser radars [9], optical atomic clocks [10], [11], ranging and remote sensing [12]. However, the performance parameters of sensitivity, precision, range, and noise of these systems depend on the span of the laser source linewidth employed [13], [14]. In light of all these, the importance of SLM-DFB laser linewidth suppression is paramount. SLM-DFB lasers operate at various wavelengths, such as at 1550 nm, 1310 nm, and 850 nm. The rugged and compact attributes of 1310 nm narrow linewidth DFB laser sources render it suitable in harsh environments for sensor and analog transmission applications [15], [16].
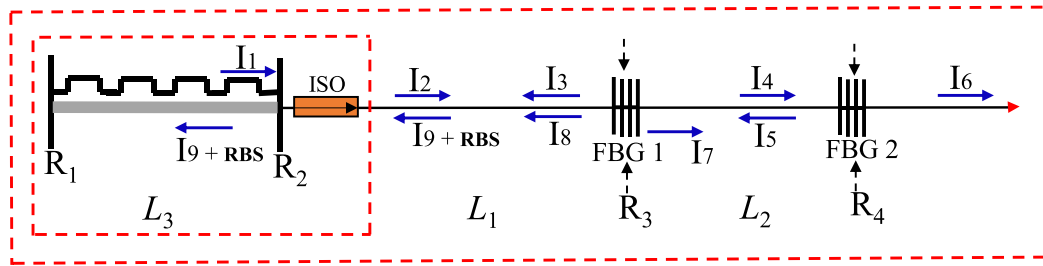
Fig. 1. Schematic of the proposed laser system based on a dual cavity fiber Bragg grating assisted feedback structure. L_3: DFB internal cavity, I_1: Internal cavity light signal, ISO: Optical isolator, L_1, L_2: Optical fiber, R_1, R_2: DFB Facet, R_3 R_4: Grating, I_2, I_4, I_6: Forward propagating light signal, I_3, I_5, I_7: FBG reflected light signal, I_8: Backward propagating light signal, $I_{9 + RBS}$: Interference backward propagating light signal accompanied by Rayleigh backscattering signal.

Over the years, there has been extensive research on achieving narrow SLM linewidth lasers. During these researches, techniques such as whispering gallery mode (WGM) resonators [17], optical self-injection feedback [18]–[23], short cavity distributed Bragg reflectors [24], microfibers [25], electrical feedback control methods [26], [27], and Rayleigh backscattering have been tested [28]–[33]. One of the successful techniques used is the coherent optical negative feedback technique, which reduces a semiconductor frequency modulation noise with the aid of an optical filter functioning as a frequency discriminator. This filter converts frequency into intensity change propagating into the laser to deeply compress the 13 MHz spectral linewidth of a DFB laser to 3 kHz. This development created a stable laser system for more than one hour, as reported in [34]. An optical circulator based self-feedback circuit and a partial reflection mirror-based feedback circuit was used to compress the several MHz spectral linewidth of a DFB-LD array to 8 kHz and 11 kHz respectively. With the utilization of a renowned self-optical feedback technique, an output power of 50 mW was attained. The difference in the outcome of the narrowed spectral linewidth was due to the partial reflection mirror-based short feedback cavity length, as reported in [35].

Currently, there is no report on an intensely compressed spectral linewidth of a 1310 nm lasing DFB laser. This paper proposes and demonstrates an idea of a laser system centered on a concept of intrinsic Lorentzian linewidth compression with a dual cavity fiber Bragg grating assisted feedback structure (DCFBGs). This structure utilizes the interference phenomenon and Vernier effect to provide optical self-injection feedback for the laser linewidth compression. It also utilizes the Rayleigh backscattering signal (RBS) as a mechanism to further compress the linewidth. The DCFBGs consists of two single-mode fibers and double FBGs, which undergo cavity overlap by the Vernier effect to enhance the side mode suppression ratio (SMSR) and maintain the DFB-SLM laser operation. The structure also broadens the free spectral range (FSR). This laser structure has proved to be stable, cost-efficient, and effectual in deep linewidth compression by three orders of magnitude. It is also capable of being employed in linewidth compression at other wavelengths. Finally, with this structure, other positive outcomes, such as the compression of the 2 MHz linewidth to ~580 Hz with an SMSR as high as 34 dB was achieved.

2. Principle and Simulation

Fig. 1 shows the principle analysis of our proposed laser system, which consists of a DFB laser and a DCFBGs. To analyze the compression principle of this system, we simplified it to a Fabry-Perot Interferometer. L_3 denotes the internal cavity of the laser diode (LD) with an internal isolator. L_1 and L_2 are conventional single-mode fibers which work with FBG 1 and FBG 2, to establish a linear optical path length. In the linear optical path, a cavity overlap of the two resonator cavities initiated by the Vernier effect of a certain ΔL cascades the two cavities together to provide optical self-injection feedback to the DFB-LD. In accordance with the Vernier Principle, L_1 was fixed, whereas

L_2 was gradually varied to achieve optimal SLM operation of our DCFBGs, which is the premise centered upon laser linewidth compression.

In this paper, for clarity, R_1, R_2, and R_3, R_4 denotes the DFB facet, and gratings respectively. Likewise, r_1, r_2, denotes the reflectivity of the DFB rear and front facet. At the same time, r_3, and r_4 denotes the reflectivity of the two gratings, respectively. The r_2, r_3 and r_4 reflectivity value taken into account in our simulation will be further discussed later on in the paper. Besides, please note that ΔL is the difference between the two fiber lengths also represented as $\Delta L = L_1 - L_2$. The propagation of optical signals in the DCFBGs is explained as, the DFB laser internal cavity lases an optical light signal I_1. This optical signal, in turn, propagates through the cavity facet and the isolator of the LD to obtain a forward propagating light signal I_2. The exit surface layer of the DFB laser named facet, shown in Fig. 1, happens to be the front mirror r_2 of the LD. After this, the light signal I_2 is divided into two signals, namely I_3, which is the reflected, and I_4, which becomes the transmitted light signal due to the reflection of FBG 1. The transmitted light signal I_4 undergoes a similar process of reflected light signal I_5 and a transmitted light signal I_6 upon arrival at FBG 2. The reflected light signal I_5, propagates and encounter FBG 1, thereby creating a reflected light signal I_7 and a transmitted light signal I_8 due to the reflection of FBG 1. The light signal I_8 undergoes a resonator cavity interference with the light signal I_3 at a region of interference phenomenon in the laser system. This interference generates a feedback light signal I_9 that continue to propagate towards the DFB laser. This interference light signal I_9 backward propagating towards the LD, is accompanied with weak RBS signal generated by the optical fiber. Therefore, we denote this signal to be $I_{9 + \mathrm{RBS}}$. The light signal $I_{9 + \mathrm{RBS}}$ of considerably small linewidth and originating from the external resonator cavity, penetrates to circulate within the DFB laser internal cavity.

The interference phenomenon occurring within our laser system, exists in a manner of a periodic variation of frequency with normalized intensity. By utilizing optical self-injection feedback, a weak RBS signal originating from the external cavity is injected into the DFB laser. Hence, laser linewidth is continually modified by the cyclic roundtrip characteristics of the weak RBS signal circulating within the DFB laser internal cavity. In turn, this further compresses the spectral linewidth of the DFB laser. The resonator cavity overlap by the Vernier effect [36], [37] arising from the impact of ΔL happens to be similar to that reported in [38]. However, the structures are different since our laser system consists of two FBGs and shorter fiber lengths.

We built a model prior to the experiment wherein numerous efforts were devoted in order to attain suitable cavity lengths. It also sought to enhance the SMSR, broaden the FSR, and investigate the laser system's sensitivity to the change in L_2 fiber length. This model considers our multi-mirror Fabry-Perot Interferometer to be a dual cavity laser structure. In our structure, the first cavity consists of R_2 and R_3, and the second cavity consists of R_3 and R_4. The transmission rates of the two cavities are shown below as [39]:

$$T_1 = \frac{(1 - r_2)(1 - r_3)}{1 + r_2 r_3 + 2\sqrt{r_2 r_3} \cos\phi_1} \tag{1}$$

$$T_2 = \frac{(1 - r_3)(1 - r_4)}{1 + r_3 r_4 + 2\sqrt{r_3 r_4} \cos\phi_2} \tag{2}$$

With the phase difference

$$\phi_1 = 2\pi \frac{2nL_1}{\lambda} \tag{3}$$

$$\phi_2 = 2\pi \frac{2nL_2}{\lambda} \tag{4}$$

in which r_2, r_3, and r_4 are the reflectivity of the three mirrors, namely the DFB front facet, grating 1, and grating 2, respectively. L_1 and L_2 denote the two-cavity lengths, n denote the refractive index. Therefore, the feedback structure can be regarded as a result of the superposition of two F-P cavities, and its transmission rate can be expressed as:
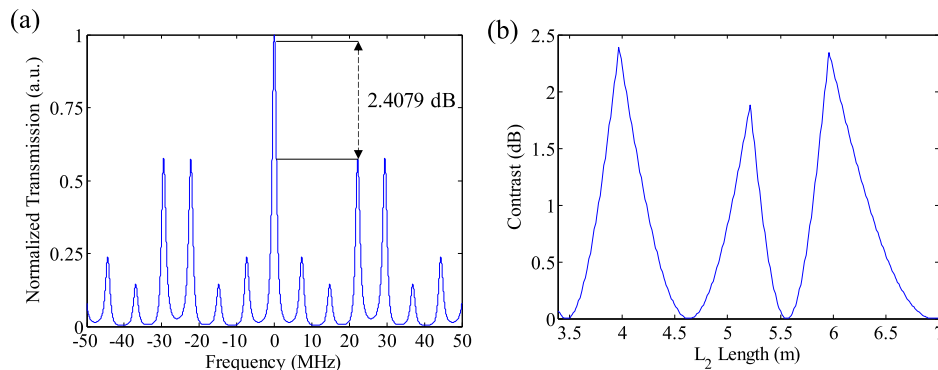
$$T = T_1 \times T_2 \tag{5}$$

Fig. 2. (a) Simulated output power when $L_1 = 13.9$ m and $L_2 = 4.0$ m. (b) Simulated output power when $L_1 = 13.9$ m and L_2 is varied.

In our simulation, $r_2 = 0.9$, $r_3 = 0.2$, and $r_4 = 0.3$. In theory, one of the transmission peaks of the two cavities needs to match the laser's wavelength, that is, the cavity length needs to satisfy the phase condition $\phi_1 = (2m_1 + 1)\pi$, $\phi_2 = (2m_2 + 1)\pi$, where m_1 and m_2 are an integer. It is indeed difficult to ensure this accuracy in the experiment. However, due to the filtering effect of the DFB laser, it's R_1 and R_2 short cavity, and the wavelength competition characteristics of the gain medium, the tendency of suppressing the side mode is feasible. In the numerical simulation, various combination of fiber lengths was investigated when the value of the resonator L_1 was fixed, whereas the value of the resonator L_2 was varied in consideration of the DFB laser benefit band. We realized that, if we set the value of L_1 to 13.9 m and the value of L_2 to 4.0 m, we are guaranteed an SLM laser system with a broad FSR, and a considerably high SMSR as seen in Fig. 2(a). The central frequency in our simulation for Fig. 2(a) did not utilize the absolute frequency value but rather had it fixed at 1310 nm. This is because our model analysis mainly strives to emphasize the function of the cavity. Hence, the cavity lengths we considered satisfies the above phase-matching conditions. Therefore, we considered how to vary L_2 to the side touch suppression ratio of the transmission spectral, which reveals the laser system's sensitivity to the change in L_2, as shown in Fig. 2(b). These resonator cavity lengths were further investigated in the experiment, and the prediction of our numerical simulation is consistent with the experiment.

3. Experimental Results and Discussion

The experimental setup to compress the linewidth of the commercial DFB laser is shown in Fig. 3. The DFB laser employed is a non-polarization maintaining output DFB laser which lases at a wavelength of 1310 nm with a 2 MHz linewidth. The 30 dB ISO is used to determine the operational direction of the laser. The ISO principle suggests that in the forward propagating direction, the transmission rate is 100%, which is the largest transmission. Likewise, in the backward direction, there is another transmission rate, which is 0.1% for the isolation of 30 dB. Therefore, just 0.1% of the reflected signal, which also consists of the weak RBS signal, propagates into the LD's internal cavity. The DFB laser is driven by a current and temperature controller (Newport Corp.) Model 6100, whose laser diode current is meticulously tuned to 24.96 mA. It is also kept at a resistance of 7.58 kΩ to coincide the two FBG central wavelengths to the DFB central wavelength. Typically, the DFB temperature sensor is always based on thermal resistance. Therefore, the temperature can be controlled by tuning the value of the resistance, which is related to the temperature sensor. In principle, a control of the temperature leads to a control of the emission wavelength. Hence, when we tune the value of the resistance on the current and temperature controller, we are practically tuning the value of its temperature. The DFB laser output power measured by a handheld optical power meter (JW3208) was found to be 4 mW. The propagating light signal originating from the DFB laser is injected into the feedback system, which consists of single-mode fiber
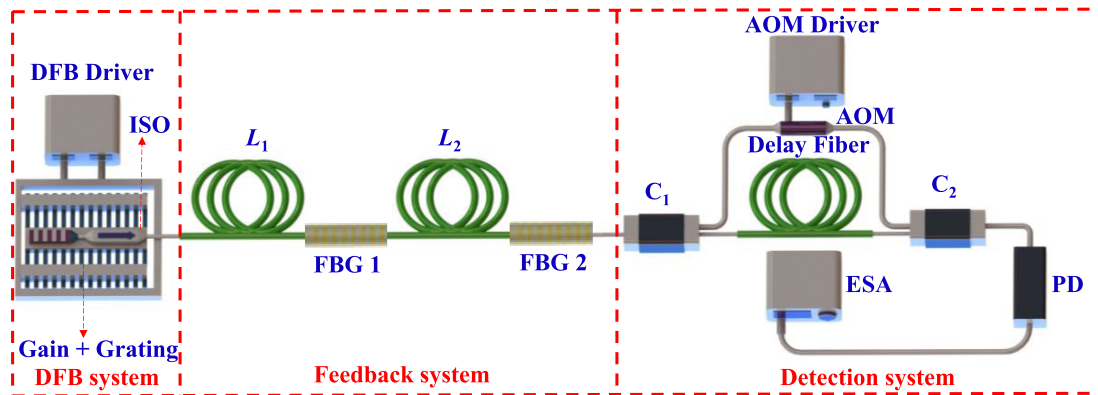
Fig. 3. Schematic of the experimental setup. ISO: optical isolator, L_1, L_2: single-mode fiber, FBG: fiber Bragg grating, C_1, C_2: fiber optic couplers, AOM: acousto-optic modulator, PD: photodetector, ESA: electrical spectrum analyzer.

−1310-XP (SMF-1310-XP) with a mode field diameter of 9.2 μm. It also has a Rayleigh scattering coefficient of −77 dB and a 0.14 numerical aperture. This study employed a single-mode fiber L_1 to sufficiently accumulate weak Rayleigh backscattering signals, which was in consideration of the backscattering capabilities of the single-mode fiber's sensitivity to an injected light power. The Rayleigh backscattering within the random distributed cascaded optical fiber L_1 is sufficiently maximized when injected power is carefully optimized. As such, one can conclude that the Rayleigh backscattering light undergoes an increase that is proportional to an injected light power increment. This Rayleigh backscattering, propagated in a circulating manner within the fiber when scattered lights at cross-sections are accumulated as weak feedback for laser linewidth compression, is a resultant of density non-uniformity within the single-mode fiber core area. This is a new technique that deeply compresses the laser linewidth and longitudinal mode selection of laser propagating in a circulating manner within the fiber as reported in Ref. [28]–[30], and also studied in our previous work Ref. [32], [33].

In addition, the feedback system also consists of an SMF named L_2 that has fiber parameters the same as L_1. It also has an FBG 1 of 20% reflectivity and an FBG 2 of 30% reflectivity. The bandwidth of the two FBGs and Bragg wavelengths are 0.148 nm and 1309.908 nm, respectively. Both FBGs with different FSR, have an equivalent central wavelength with a weak Rayleigh scattering situated at this central wavelength. The cavity overlap between the two-feedback resonator cavities by the Vernier effect cascades the side modes and enhances the central wavelength to obtain a high SMSR and broaden FSR. These two FBGs whose bandwidth is larger than 10 GHz, suggests that the filtering effect of the FBGs should not contribute to the linewidth compression. This is because a filtering bandwidth of 0.148 nm corresponding to FBG 1 and FBG 2, is larger than 10 GHz. Nonetheless, these two FBGs were used to provide the reflectance to compress the linewidth initially, and further helped maintain the stability of the deep linewidth compression induced by the RBS signal. The insertion loss in our feedback system mainly originates from the two gratings, whereas other points of connection along the feedback system are fusion spliced together using a fusion splicer (Fitel S178 A). The first cause of insertion loss is the splicing loss between the fibers. The second cause of insertion loss originates from the FBG, which is associated with the fact that we did not require a full reflectance of 100%. The actual reflectance of each FBG, which is 20% and 30%, can characterize the insertion loss. We adopted a standard telecommunication SMF fiber, which rendered the transportation insertion loss of the optical fiber to be very low. Therefore, the actual insertion loss between each component in our laser system is less than 1 dB.

Conclusively, in our laser system, spectral laser linewidth compression can be categorized as an origination from two aspects. The first aspect is the Vernier effect and light signal interference mode suppression of the cavities in the dual-cavity FBG system. Whereas the second aspect is the
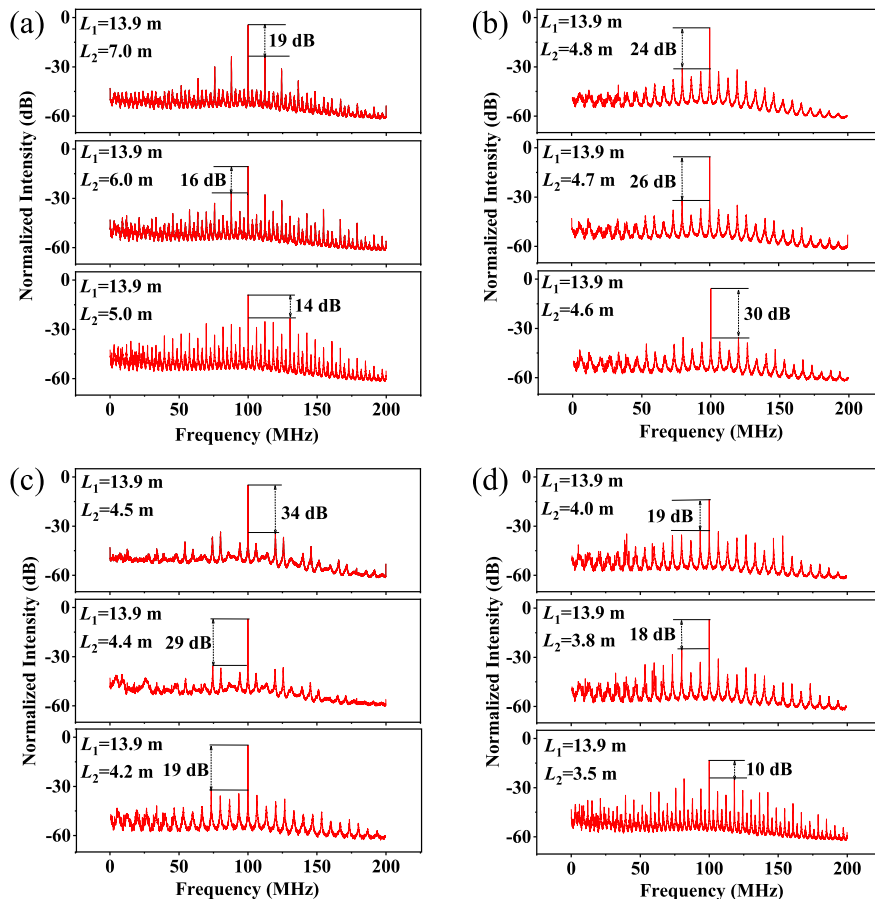
Fig. 4. (a)–(d) Effective detected normalized power spectra for selected different combinations of feedback lengths with DCFBGs.

RBS signal accompanied in the fibers. Although the dual cavity compression effect can compress the linewidth to approximately 1 kHz, however, case scenarios such as ours that seeks further compression to a sub-kHz level, the Rayleigh backscattering effect serves to be of substantial impact. Therefore, the laser linewidth was compressed by employing double FBGs to construct an optical self-injection feedback dual cavity fiber structure. Furthermore, this structure generates a weak RBS signal with characteristics of a controlled weak feedback power and a continually narrowing effect in the frequency domain. When the two feedback cavities overlap by the Vernier effect, the central wavelength of the FBG and fiber will cascade into an equivalent wavelength in the frequency domain. This ultimately renders the Rayleigh scattering to be centered at the central cascaded wavelength, and further allows the RBS to undergo a continuous circulation over the gain threshold of the DFB laser. As a resultant of the narrow-bandwidth filtering characteristics of Rayleigh scattering, the laser linewidth is continually modified by the cyclic roundtrip characteristics of the RBS signal circulating within the DFB laser internal cavity. This phenomenon progressively occurs until laser outputs reach dynamic equilibrium, which ultimately further compressed the spectral linewidth of the laser to a sub-kHz. A Self-coherent envelope linewidth detection method (SCELD) with a 2 km delaying fiber, an Acousto optical modulator (AOM) frequency shift of 100 MHz, and a Photodetector (PD) of 350 MHz is used to measure the laser linewidth [40], [41].

    Fig. 4(a–d) shows the impact of the L_2 fiber length on the system output laser side mode when L_1 remains unchanged. When L_2 is set to 7 m, 6 m, and 5 m, the FSR appears to be narrow. More side modes oscillate in a manner of gradual, continuous mode hopping that competes with
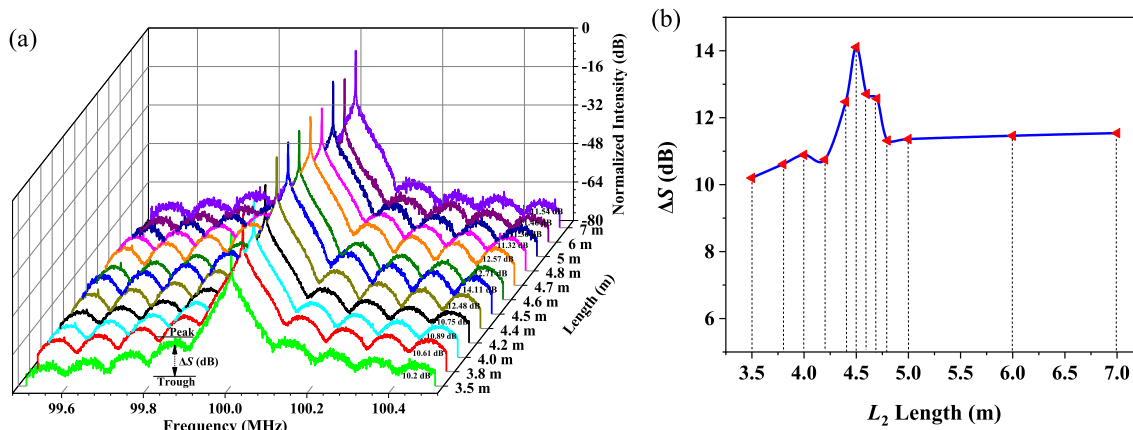
Fig. 5. (a) Effective detected normalized power spectra for selected different combinations of feedback lengths with DCFBGs. (b) Detected laser linewidth as a function of feedback length L_2.

the main longitudinal mode. The longitudinal mode of the dual cavity is short, and it results in a vast and dense cavity mode overlap with SMSR of 19 dB, 16 dB, and 14 dB for the 7 m, 6 m, and 5 m, respectively. When L_2 is decreased to 4.8 m, the FSR broadens. The longitudinal mode spacing of the two cavities at this length increases, and the side modes at the edges are less and weaker in comparison to an L_2 of 7 m, 6 m, and 5 m. The output spectrum begins to display a distinct mode overlap shape with an SMSR of 24 dB. With these considerations, this study gradually reduced L_2 by one-meter. We observed a slight increment in SMSR of 26 dB and 30 dB across feedback cavity lengths of 4.7 m and 4.6 m, respectively. This encouraged further decrement to attain sufficient SMSR. When L_2 was decreased to 4.5 m, we realized that such a phase length achieved an ideal optimal value whose edge mode is relatively weaker than 4.8 m, 4.7 m, and 4.6 m. At this length, an SMSR of 34 dB was attained. When L_2 was further decreased to 4.4 m and 4.2 m, we observed that more side modes begin to oscillate at 4.2 m, whose distinctive cavity overlap was gradually disappearing. We observed a decline in SMSR from an optimal value down to 29 dB and 19 dB for the 4.4 m and 4.2 m, respectively. This steady decline was observed across the cavity length of 4.0 m, 3.8 m, and 3.5 m, wherein the side modes were relatively denser. These results proved a progressive setback in the quest to attain a stable SLM output laser. We concluded that the overlap of the two-cavity mode for these lengths is too small, resulting in a dense output laser side mode and no apparent mode overlap shape. In addition, we observed a gradual mode-hopping with SMSR of 19 dB, 18 dB, for 4.0 m, and 3.8 m, respectively. Likewise, an overwhelming mode-hopping at 3.5 m whose SMSR is 10 dB and its modes oscillate in a manner of continuous progressive mode hopping that competes with the main longitudinal mode. Certainly, the laser is operating at a state of multi-mode for these lengths. Based on Fig. 4(a–d), we fixed the resonator cavity L_1 to 13.9 m and meticulously varied the length of L_2. As a result, we positively identified the optimal length for L_2 to be within the range of 4.0 m-4.8 m in our work.

Fig. 5(a) shows the normalized power spectrum for different feedback lengths. As the length of L_1 is fixed and L_2 is varied, the detected output linewidth changes appropriately. The laser linewidth progressively compresses as the length of L_2 changes, which suggests that longer feedback lengths support laser linewidth compression. However, Fig. 4(a–d) indicate that longer lengths lead to smaller FSR, density in side modes, and difficulty in ascertaining the laser's SLM operation. In this regard, the length of L_2 ought to be carefully selected. The study also observed a steady, gradual increment between the peak and trough of the coherent envelope, ranging from the green curve until the blue curve, just before a steady decline occurred from the blue curve until the violet curve. It is observable that when the length of L_2 is 4.5 m, the peak and trough are stable and higher than in other curves. In theory, a long single-mode fiber is suitable for the accumulation of Rayleigh backscattering for laser linewidth compression. We anticipate that
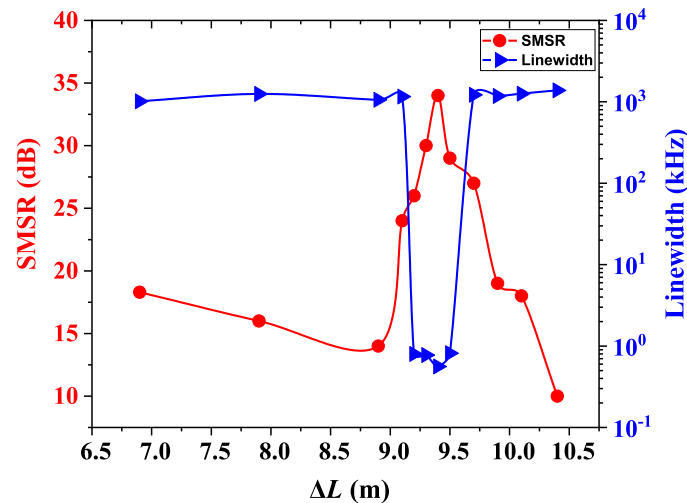
Fig. 6. The SMSR (Red points) from the detected normalized power spectra and their corresponding linewidth (Blue points) from the SCELD measurements wherein $\Delta L = L_1 - L_2$.

a long optical path length after roundtrip time will be proficient at generating weak optical feedback signal suitable for linewidth compression. This is feasibly arising from its efficiency to generate constructive interference for optical light signals of long coherence length. However, a feedback cavity that is too long induces more noise to the system, whereas a cavity that is too short fails to accumulate sufficient Rayleigh backscattering signal. Therefore, a resonator cavity length, which is neither too long nor too short, remains suitable for laser linewidth compression due to its shorter roundtrip time. Even then, however, the ideal length ought to be carefully selected to attain deep laser linewidth compression and stability.

The amplitude difference comparison of coherent envelope method (ADCCE) is used to measure the linewidth of the detected laser precisely, as shown in Fig. 5(a) and 5(b) Ref. [40]. The mathematical symbol ΔS is a value obtained by comparing the contrast difference between the second peak and the second trough (CDSPST) of the coherent envelope of the power spectral. It uses a short delay fiber of 2 km. This value is needed to characterize an accurate laser linewidth that is below 1 kHz while utilizing the ADCCE method as employed in our experiment. Hence the reported laser linewidth of ∼580 Hz only at a high value of 14.11 dB, as shown in Fig. 5(b). Likewise, as the length gradually increases to 4.6 m, a ΔS of 12.71 dB that corresponds to a laser linewidth of 774 Hz, is attained. Laser linewidth gradually declines even at a length of 4.7 m, where a ΔS of 12.57 dB (800 Hz) was attained. This decrement in laser linewidth appeared to be on a progressive decline for an L_2 feedback cavity length of 4.8 m, 5 m, 6 m, and 7 m, whose linewidths are 1.161 kHz, 1.057 kHz, 1.250 kHz, and 1.214 kHz respectively. Likewise, when L_2 was set to 3.5 m, a ΔS of 10.2 dB that correspond to a laser linewidth of 1.381 kHz was attained. The laser linewidth at this point gradually increased across L_2 of 3.8 m, 4.0 m, 4.2 m, and 4.4 m whose value of ΔS and linewidth are 10.61 dB (1.256 kHz), 10.89 dB (1.178 kHz), 10.75 dB (1.216 kHz), and 12.48 dB (816 Hz) respectively. The above phenomenon is in accordance with the theory of a too-long length and a too-short length that leads to a low value of linewidth, narrowed FSR, small SMSR, and difficulty in attaining SLM operation of the laser as shown in Fig. 4(a, b, c, d).

Fig. 6 shows the curves change law for the SMSR and its corresponding linewidth for different ΔL. For clarity, please note that ΔL on the x-axis in the above figure is the difference between the two fiber lengths, also represented as $\Delta L = L_1 - L_2$. When ΔL is small, which entails L_1 and L_2 approaches an equal length, a small SMSR, and laser linewidth is shown. As ΔL increases, the linewidth gradually compresses, and the SMSR increases as seen at a ΔL of 9.1 m. When ΔL was within the range of 9.2 m to 9.3 m, we observed a compressed laser linewidth that was less than 1 kHz, thereby suggesting that our DCFBGs is gradually operating at our desired optimal
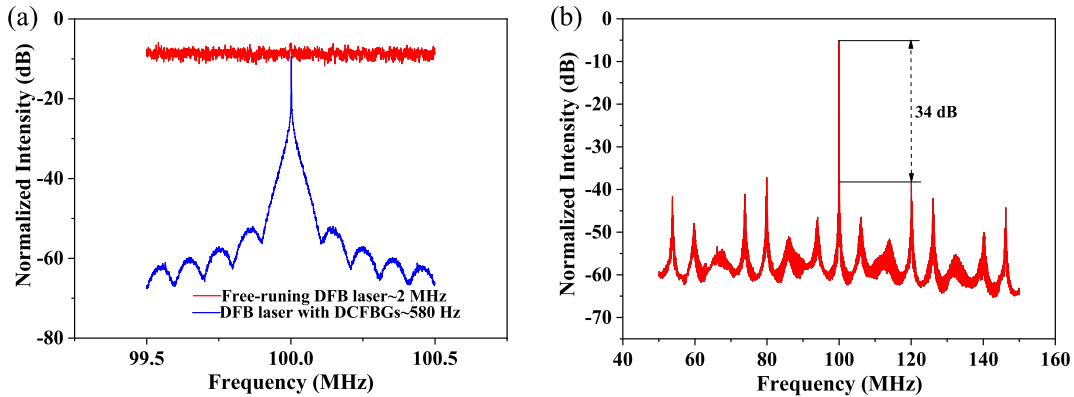
Fig. 7. (a) Normalized power spectra of free running DFB laser (red line) and DFB laser with DCFBGs (blue line). (b) Output power spectra when $L_1 = 13.9$ m and $L_2 = 4.5$ m.

level. We only attained a suppressed side mode and SMSR of 34 dB at a $\triangle L$ of 9.4 m, which is in accordance with the fact that a single longitudinal mode operation is the precondition of laser linewidth compression. In this instance, the linewidth of 580 Hz was compressed, arising from a sufficient gain at the main lasing mode.

However, a further progressive increase in $\triangle L$ resulted in a steady deterioration in SMSR and linewidth. In principle, therefore, the FSR considered to be the mode spacing in frequency or wavelength for the forward and backward propagating light signal in our laser system is expressed as [42]:

$$FSR = \frac{c}{2n(L_1 - L_2)} \tag{6}$$

where c is the speed of light, the coefficient 2 indicates the signal traverse forward and backward, n is the refractive index, L_1, and L_2 are the phase length. Ultimately, a small $\triangle L$ broadens the FSR and attains the SLM operation of our laser system by utilizing the Vernier principle which suggests one cavity length serves as a threshold length, whereas the other cavity length is meticulously tuned to initiate the Vernier effect. Therefore, it is imperative that a suitable $\triangle L$ is employed in order to suppress case scenarios of mode overlapping and attain a laser system of high SMSR and well broaden FSR. Because there exists a tendency where a substantially small or large $\triangle L$ initiates a resonator cavity overlap for our DCFBGs that generates new side modes hindering the feasibility of attaining a considerably high SMSR as reported in Fig. 6.

A delay self-heterodyne system (DSHS) with a 2 km delaying fiber and a 100 MHz AOM frequency shift is used to observe SLM and accurately measure the laser spectral linewidth with and without the DCFBGs Ref. [40], [41]. The main difference in comparison to the traditional delayed self-heterodyne interferometry (DSHI) method, is that, our method required the delay fiber to be much shorter than the coherent length of the narrow linewidth laser under test (LUT). This is essential in order to obtain the oscillatory coherent envelope in the spectral of the optical beat. We discovered the laser linewidth was compressed from 2 MHz to ∼580 Hz, as shown in Fig. 7(a). Furthermore, an SMSR of 34 dB with a finely broad FSR and an ideal SLM operation of the DFB laser at a frequency span of 100 MHz was achieved when two feedback lengths were set to 13.9 m and 4.5 m as shown in Fig. 7(b). Hence, our laser system and its principle of operation utilize the interference phenomenon, Vernier effect, and RBS signal.

The feedback system's output power stability was measured using an optical spectrum analyzer (OSA) (AQ6370D, YOKOGAWA) with a 0.02 nm resolution after every five-minute interval. The output power slightly increases to 2.04 mW within the first five minutes of the laser and maintains an output power of 2.0 mW throughout the next forty minutes. As shown in Fig. 8(a), the maximum output power of our DCFBGs was found to be stable at 2.0 mW. The frequency noise power
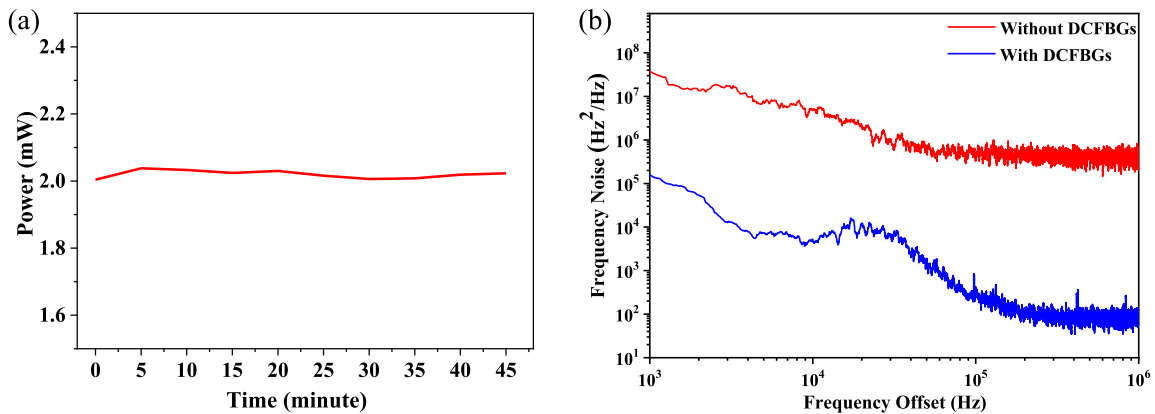
Fig. 8. (a) Output power stability of DCFBGs. (b) Frequency noise power spectra density of the DFB laser with and without DCFBGs.

spectral density (PSD) of the DFB laser with and without DCFBGs is shown in Fig. 8(b), wherein the frequency noise of the laser was measured by an unbalanced Michelson interferometer with a 10 m optical path difference (OPD) and a delay fiber of 5 m. This method was successfully applied in other works, Ref. [24]. According to the Nyquist law, Δt directly determines the measured frequency upper limit of the frequency noise. To approximate the original differential of the laser phase accurately, we employed a 5 m delay fiber to induce a Δt of $5 \times 10^{-8}s$, which can measure the frequency noise high to 1 MHz. In comparison to the DFB laser without the DCFBGs represented by the red curve, the frequency noise power spectral density of the DFB laser with the DCFBGs represented by the blue curve is suppressed by three orders of magnitude. The output spectral linewidth of the DFB laser with the DCFBGs can be estimated to be approximately 550 Hz [43], which is close to the linewidth value (580 Hz) measured by the SCELD.

The DFB laser we employed was a non-polarization maintaining laser. For further improvements, a polarization-maintaining DFB laser can be employed. In order to suppress the influence of polarization, the components of the feedback system, precisely the single-mode fiber, can be replaced with a polarization-maintaining fiber (PMF). Such a replacement will help maintain mode overlapping for feedback cavity lengths L_1 and L_2. The limitation of our laser linewidth is dependent on the DFB temperature controller employed to maintain a frequency shift. Hence, the DFB temperature controller needs to be meticulously tuned to suitable power and kept at an appropriate temperature with the utilization of vibration isolation to reduce wavelength shift. Provided PMF devices are employed to guarantee laser stability and reduce the influence of $1/f$ noise, a deeply compressed laser spectral linewidth to an order of 100 Hz is feasible.

Optimization of the feedback structure FBGs in terms of fabrication to improve the performance level of bandwidth and reflectivity, a deep spectral linewidth compression, and high SMSR in contrast to ours is feasible. Such optimization is valid since the reflectance of the FBGs interferes with the DFB laser lasing injected pulse. A VOA (variable optical attenuator) can be attached between the Rayleigh scattering fiber and the FBG to adjust the injected laser forward propagating light intensity and the accumulated RBS light signal within the fiber. These adjustments also help to reduce cavity loss and suppress side modes. Integration of the laser chip, FBGs, and all other fabricated devices into one waveguide ensures that issues relating to laser stability, and temperature control can be resolved. In order to obtain a profoundly narrowed spectral laser linewidth, we can package the laser system by leveraging the shockproof and thermostatic technology to enhance the stability of the output laser system.

4. Conclusion

This study proposed, simulated, and experimentally demonstrated a DCFBGs effective enough to provide weak optical feedback to deeply compress the intrinsic Lorentzian spectral linewidth of a 1310 nm DFB laser, with SMSR enhanced and FSR broadened. This was feasible by utilizing the Vernier effect, interference phenomenon, and Rayleigh backscattering mechanism. The DFB 2 MHz linewidth was intensely compressed to ~580 Hz with a side mode suppression ratio of 34 dB at an output power stability of 2.0 mW. The frequency noise of the DFB laser with the DCFBGs was significantly suppressed by three orders of magnitude. This high-quality laser finds versatile applications in optical fiber communication and optical fiber sensing fields where an ultra-narrow linewidth is of high demand.

References

[1] R. Passy, N. Gisin, J. P. von der Weid, and H. H. Gilgen, "Experimental and theoretical investigations of coherent OFDR with semiconductor laser sources," *J. Lightw. Technol.*, vol. 12, no. 9, pp. 1622–1630, Sep. 1994.

[2] M. Harris, G. N. Pearson, J. M. Vaughan, D. Letalick, and C. Karlsson, "The role of laser coherence length in continuous-wave coherent laser radar," *J. Modern Opt.*, vol. 45, no. 8, pp. 1567–1581, 1998.

[3] N. C. Pixley, T. L. Correll, D. Pappas, O. I. Matveev, B. W. Smith, and J. D. Winefordner, "Tunable resonance fluorescence monochromator with sub-Doppler spectral resolution," *Opt. Lett.*, vol. 26, no. 24, pp. 1946–1948, 2001.

[4] G. A. Cranch, P. J. Nash, and C. K. Kirkendall, "Large-scale remotely interrogated arrays of fiber-optic interferometric sensors for underwater acoustic applications," *IEEE Sens. J.*, vol. 3, no. 1, pp. 19–30, Feb. 2003.

[5] J. Geng, C. Spiegelberg, and S. Jiang, "A compact 100-km FMCW fiber laser radar," in *Proc. Quantum Electron. Laser Sci. Conf.*, 2005, pp. 1983–1985.

[6] L. L. Shi, T. Zhu, Q. He, and S. H. Huang, "Effect of laser linewidth on phase-OTDR based distributed vibration sensing regime," in *Proc. 23rd Int. Conf. Opt. Fibre Sens.*, 2014, Art. no. 91576H.

[7] I. Coddington *et al.*, "Coherent optical link over hundreds of metres and hundreds of terahertz with subfemtosecond timing jitter," *Nature Photon.*, vol. 1, pp. 283–287, 2007.

[8] E. Ip, A. P. T. Lau, D. J. F. Barros, and J. M. Kahn, "Coherent detection in optical fiber systems," *Opt. Express*, vol. 16, no. 2, pp. 753–791, 2008.

[9] H. Edner, A. Sunesson, and S. Svanberg, "NO plume mapping by laser-radar techniques," *Opt. Lett.*, vol. 13, no. 9, pp. 704–706, 1988.

[10] B. Argence *et al.*, "Quantum cascade laser frequency stabilization at the sub-Hz level," *Nature Photon.*, vol. 9, pp. 456–460, 2015.

[11] A. D. Ludlow *et al.*, "Systematic study of the 87Sr clock transition in an optical lattice," *Phys. Rev. Lett.*, vol. 96, no. 033003, 2006.

[12] E. C. Burrows, and K. Y. Liou, "High resolution laser LIDAR utilising two-section distributed feedback semiconductor laser as a coherent source," *Electron. Lett.*, vol. 26, no. 9, pp. 577–579, 1990.

[13] W. Zeller, L. Naehle, P. Fuchs, F. Gerschuetz, L. Hildebrandt, and J. Koeth, "DFB lasers between 760 nm and 16 μm for sensing applications," *Sensors*, vol. 10, no. 4, pp. 2492–2510, 2010.

[14] G. Bonfrate, F. Vaninetti, and F. Negrisolo, "Single-frequency MOPA Er/sup 3+/ DBR fiber laser for WDM digital telecommunication systems," *IEEE Photon. Technol. Lett.*, vol. 10, no. 8, pp. 1109–1111, Aug. 1998.

[15] P. Doussiere, C. L. Shieh, S. DeMars, and K. Dzurko, "Very high power 1310 nm InP single mode distributed feedback laser diode with reduced linewidth," in *Proc. Novel In-Plane Semicond. Lasers VI*, vol. 6485, 2007, Art. no. 64850G.

[16] J. Jewell, L. Graham, M. Crom, K. Maranowski, J. Smith, and T. Fanning, "1310 nm VCSELs in 1-10Gb/s commercial applications," in *Proc. Vertical-Cavity Surface-Emitting Lasers X*, vol. 6132, 2006, Art. no. 613204.

[17] W. Liang *et al.*, "Ultralow noise miniature external cavity semiconductor laser," *Nature Commun.*, vol. 6, no. 7371, 2015.

[18] F. Kéfélian, H. Jiang, P. Lemonde, and G. Santarelli, "Ultralow-frequency-noise stabilization of a laser by locking to an optical fiber-delay line," *Opt. Lett.*, vol. 34, no. 7, pp. 914–916, 2009.

[19] Q. Lin, M. A. V. Camp, H. Zhang, B. Jelenkovic, and V. Vuletic, "Long-external-cavity distributed Bragg reflector laser with subkilohertz intrinsic linewidth," *Opt. Lett.*, vol. 37, no. 11, pp. 1989–1991, 2012.

[20] X. Huang *et al.*, "Linewidth suppression mechanism of self-injection locked single-frequency fiber laser," *Opt. Express*, vol. 24, no. 17, pp. 18907–18916, 2016.

[21] D. Brunner, R. Luna, A. Delhom i Latorre, X. Porte, and I. Fischer, "Semiconductor laser linewidth reduction by six orders of magnitude via delayed optical feedback," *Opt. Lett.*, vol. 42, no. 1, pp. 163–166, 2017.

[22] F. Wei *et al.*, "Subkilohertz linewidth reduction of a DFB diode laser using self-injection locking with a fiber Bragg grating Fabry-Perot cavity," *Opt. Express*, vol. 24, no. 15, pp. 17406–17415, 2016.

[23] H. Ishii *et al.*, "Narrow linewidth tunable DFB laser array integrated with optical feedback planar lightwave circuit (PLC)," *IEEE J. Sel. Top. Quantum Electron.*, vol. 23, no. 6, pp. 1–7, Nov. /Dec. 2017.

[24] C. Spiegelberg, J. Geng, Y. Hu, Y. Kaneda, S. Jiang, and N. Peyghambarian, "Low-noise narrow-linewidth fiber laser at 1550 nm," *J. Lightw. Technol.*, vol. 22, no. 1, pp. 57–62, Jan. 2004.

[25] W. Fan, J. Gan, Z. Zhang, X. Wei, S. Xu, and Z. Yang, "Narrow linewidth single frequency microfiber laser," *Opt. Lett.*, vol. 37, no. 20, pp. 4323–4325, 2012.

[26] M. Ohtsu, M. Murata, and M. Kourogi, "FM noise reduction and sub-kilohertz linewidth of an AlGaAs laser by negative electrical feedback," *IEEE J. Quantum Electron.*, vol. 26, no. 2, pp. 231–241, Feb. 1990.

[27] M. Poulin *et al.*, "Compact narrow linewidth semiconductor laser module," in *Proc. Laser Technol. Defense Security V*, vol. 7325, 2009, Art. no. 73250O.

[28] T. Zhu, S. H. Huang, L. L. Shi, W. Huang, M. Liu, and K. S. Chiang, "Rayleigh backscattering: A method to highly compress laser linewidth," *Chinese Sci. Bulletin*, vol. 59, pp. 4631–4636, 2014.

[29] T. Zhu, F. Y. Chen, S. H. Huang, and X. Y. Bao, "An ultra-narrow linewidth fiber ring laser based on Rayleigh backscattering in a tapered optical fiber," *Laser Phys. Lett.*, vol. 10, no. 5, pp. 79–83, 2013.

[30] T. Zhu, X. Bao, L. Chen, H. Liang, and Y. Dong, "Experimental study on stimulated Rayleigh scattering in optical fibers," *Opt. Express*, vol. 18, no. 22, pp. 22958–22963, 2010.

[31] G. Yin, B. Saxena, and X. Y. Bao, "Tunable Er-doped fiber ring laser with single longitudinal mode operation based on Rayleigh backscattering in single mode fiber," *Opt. Express*, vol. 19, no. 27, pp. 25981–25989, 2011.

[32] F. Li, T. Lan, L. Huang, I. P. Ikechukwu, W. Liu, and T. Zhu, "Spectrum evolution of Rayleigh scattering in one-dimensional waveguide," *Opto-Electron. Adv.*, vol. 02, no. 08, 2019, Art. no. 190012.

[33] F. Li *et al.*, "Rayleigh scattering assisted ultra-narrow linewidth linear-cavity laser," *Appl. Phys. Express*, vol. 12, no. 8, 2019.

[34] K. Aoyama, N. Yokota, and H. Yasaka, "3-kHz spectral linewidth laser assembly with coherent optical negative feedback," *IEEE Photon. Technol. Lett.*, vol. 30, no. 3, pp. 277–280, Feb. 2018.

[35] K. Kasai, M. Nakazawa, M. Ishikawa, and H. Ishii, "8 kHz linewidth, 50 mW output, full C-band wavelength tunable DFB LD array with self-optical feedback," *Opt. Express*, vol. 26, no. 5, pp. 5675–5685, 2018.

[36] L. Li, M. Zhang, Y. Liu, Y. Li, and Y. Wang, "Stable single-longitudinal-mode erbium-doped fiber laser with narrow linewidth utilizing parallel fiber ring resonator incorporating saturable absorber and fiber Bragg grating," *Appl. Opt.*, vol. 54, no. 13, pp. 4001–4005, 2015.

[37] M. Li *et al.*, "Single mode compound microsphere laser," *Opt. Commun.*, vol. 120, pp. 1–5, 2018.

[38] S. H. Huang *et al.*, "Dual-cavity feedback assisted DFB narrow linewidth laser," *Scientific Rep.*, vol. 7, 2017, Art. no. 1185.

[39] Y. O. Barmenkov, D. Zalvidea, S. Torres-Peiró, J. L. Cruz, and M. V. Andrés, "Effective length of short Fabry-Perot cavity formed by uniform fiber Bragg gratings," *Opt. Express*, vol. 14, no. 14, pp. 6394–6399, 2006.

[40] S. H. Huang *et al.*, "Laser linewidth measurement based on amplitude difference comparison of coherent envelope," *IEEE Photon. Technol. Lett.*, vol. 28, no. 7, pp. 759–762, Apr. 2016.

[41] S. H. Huang, T. Zhu, M. Liu, and W. Huang, "Precise measurement of ultra-narrow laser linewidths using the strong coherent envelope," *Scientific Rep.*, vol. 7, 2017, Art. no. 41988.

[42] X. X. Yang, L. Zhan, Q. S. Shen, and Y. X. Xia, "High-power single-longitudinal-mode fiber laser with a ring Fabry–Pérot resonator and a saturable absorber," *IEEE Photon. Technol. Lett.*, vol. 20, no. 11, pp. 879–881, Jun. 2008.

[43] G. D. Domenico, S. Schilt, and P. Thomann, "Simple approach to the relation between laser frequency noise and laser line shape," *Appl. Opt.*, vol. 49, no. 25, pp. 4801–4807, 2010.